ESEM Studies of Colloidal Sulfur Deposition in a Natural Microbial Community from a Cold Sulfide Spring Near Ancaster, Ontario, Canada

Susanne Douglas*[1] and Dean D. Douglas[2]

[1]Astrobiology Research Element, NASA Jet Propulsion Laboratory,
4800 Oak Grove Dr., Pasadena, CA 91109
[2]Department of Microbiology,
University of Guelph, Guelph, Ont. N1G 2W1, Canada

*To whom correspondence should be addressed. Email: Susanne.Douglas@jpl.nasa.gov
Phone: (818)354-6322; Fax: (818)393-4445

ABSTRACT

We have used a relatively new microscopical technique, environmental scanning electron microscopy (ESEM), together with transmission electron microscopy (TEM) and light microscopy to investigate a unique microbial community from a temperate climate, cold sulfide spring near Ancaster, Ontario, Canada. ESEM allows the viewing of fully hydrated specimens which have not been structurally or chemically altered by the extensive procedures necessary to allow biological specimens to be viewed in a vacuum. In addition to allowing visualisation of microorganisms in their natural form and as intact assemblages, ESEM also allows detection of elements especially those lighter than Si, which tend to be lost or masked by the processes used to prepare samples for conventional SEM and for TEM thin sections. In this study we report new information regarding the structure of bacteriogenic sulfur deposits and their relationship to the structural aspects of a natural microbial community from a cold sulfide spring near Ancaster, Ontario, Canada.

INTRODUCTION

Most bacteria in nature live as part of dynamic metabolically interactive assemblages which can be found covering most solid substrates (rocks, plants, man-made structures) in almost every environment on Earth. Almost 90% of all microorganisms live as part of such assemblages, commonly referred to as biofilms (Douglas and Beveridge 1998). In extreme environments where conditions of temperature, pH, or nutrient scarcity are so harsh as to eliminate grazing organisms, these biofilms can often grow very thick (up to tens of centimetres) and are then often referred to as microbial mats. In mats, the cells are enveloped within a highly hydrated extracellular polymeric matrix (EPS) which they create. EPS serves many protective purposes and determines the structural fabric and spatial arrangement of cells within the community. All the organisms will position themselves in the regions where they can fulfil their own specific chemical and physical requirements so that the communities are often structured very precisely along particular chemical gradients (Jørgensen and Cohen 1977; D'Amelio et al. 1989).

The present study describes a subpopulation, the sulfide oxidising bacteria, of a microbial mat community from a cold sulfide spring located near Ancaster, Ontario, Canada. This spring has not been described previous to our studies (Douglas and Douglas, in prep.) but provides a fascinating opportunity to study the interactions between microorganisms and geochemistry in a well-developed microbial community. The mats line and choke the source of the spring, from which sulfide-rich water flows at a rapid rate to follow the bottom of a ravine. The highly reduced waters of the source host multi-coloured mats of blue-green (cyanobacteria) to brownish green (green sulfur bacteria) with interspersed pink (purple sulfur bacteria) and white patches (mainly cell-associated bacteriogenic sulfur deposits). Where the water pours over the lip of the source pool, it becomes oxygenated and

the dominant mat colour changes from dark rich tones to white (colourless sulfur oxidising bacteria and associated bacteriogenic sulfur) due to extensive microbial growth on the channel bottom as organisms continue to utilise the reduced sulfur for energy. This is an extended down-gradient version of the well known coloured laminations seen in microbial mats from other sulfide-rich environments, particularly marine intertidal areas. The different colours arise from the presence of dominant microbial groups flourishing in their preferred niches within the sulfide-oxygen gradient. Many other complicating factors come into play in determining the positioning of the microorganisms such as the availability of light and other needed nutrients such as iron.

One of the aspects of sulfide community structure that has been difficult to study has been the relationship between sulfide oxidising bacteria and sulfur deposits ("elemental sulfur"). Most electron microscopical techniques destroy or markedly change such deposits while light microscopical techniques generally lack the resolving power to allow details to be seen. With the use of environmental scanning electron microscopy (ESEM), we were able to view fully hydrated, chemically unaltered samples and to determine some interesting, previously unconfirmed aspects of the relationship between microorganisms and elemental sulfur deposits, both intracellular and extracellular.

MATERIALS AND METHODS

Sample collection. Samples were collected by scooping mat material into sterile 21-mL borosilicate vials and filling to the top with water from the spring itself to preserve the anoxic character of the sample. Mats from different regions within the spring had different colours depending

on the dominant group of organisms and two samples of each colour was collected. Of each pair, one was left undisturbed while the other was used to take samples for microscopy. The vials were kept at 20°C in natural light since no lighted cold chambers were available. No colour changes (indicating major population change) took place during the course of the study.

Environmental scanning electron microscopy (ESEM). Small (about 5mm diameter) pieces of living mat were removed from sample vials immediately prior to viewing in the ESEM using sterile forceps and placed on 25 mm diameter 0.22μm pore size polycarbonate filters. The filters served as a supporting substrate and were kept hydrated by placing them on wet Whatman No. 2 filter paper within closed glass Petri dishes. In this way the samples were transported to the microscope. For viewing, small pieces of the filters, holding the mat material, were cut out and placed on 1-cm diameter cylindrical metal slugs using double-sided carbon tape. These were placed within a metal cup in the Peltier stage and provided thermal coupling to the stage temperature controller.

All images were collected using a Philips XL30 ESEM equipped with a field emission electron gun. Within the ESEM, mat samples were kept at a temperature of 3°C using the Peltier cooling stage. The water vapour pressure was set at 5.4 Torr, giving a relative humidity in the sample chamber of 95%. This level was chosen through trials which showed that it allowed full hydration of the specimen but with only a thin film of water present so that detailsm could be seen. Accelerating voltage was set at 20 keV and images were collected digitally using the ESEM software.

Energy dispersive x-ray spectroscopy (EDS). The ESEM was equipped with a Princeton-GammaTech energy dispersive x-ray spectrometer optimised for light element detection. The instrumentation allowed bulk elemental composition to be determined as well as relative atomic proportions within the sample. In addition, the EDS system can interface to the imaging capabilities

of the ESEM, allowing the production of elemental maps.

X-ray collection was performed using an accelerating voltage of 20 keV for 100s live time. This generally allowed a total count of 100 000 to be achieved with good spectral resolution. Under these conditions, using "spot mode" to collect xrays from specific points in the sample, and beam penetration into the sample was at most 1-2 μm based on a Monte Carlo simulation with Si as the matrix material. "Standardless" quantitative analysis allowed estimates of relative proportions of elements to be made within an error margin of 0.1%.

X-ray maps were collected under the same conditions as individual spectra except that they were collected for 3600s live time to allow a clear image to be obtained.

Transmission electron microscopy. Mat sections were placed in 7-mL borosilicate sample vials with spring water and 25% aqueous glutaraldehyde was added to give a final concentration of 3% (v/v). The glutaraldehyde-fixed mat pieces were left in glutaraldehyde for at least 24 h at 4°C, washed with ultrapure water, and then post-fixed in 2% (w/v) OsO_4 for 2 hours at room temperature. After washing again, the mats were exposed to a solution of 2% (w/v) aqueous uranyl acetate for 30 min before dehydration. The samples were gradually dehydrated through immersion in a series of ethanol solutions to 100% ethanol. This was followed by 50:50 ethanol:acetone, and 100% acetone. Each step was carried out at room temperature (22°C) for 15 min. The samples were then covered with a 50:50 mixture of acetone:Epon 812 resin (Can-Em, Guelph, ON) and left overnight in order to allow infiltration of the cells by Epon. After embedding in fresh Epon, they were polymerised at 60°C for 48 hours. Thin sections (60-70 nm) were cut using a Reichert-Jung Ultracut E ultramicrotome equipped with a diamond knife.

For ultrastructural evaluation of the samples, the sections were mounted on carbon- and

Formvar-coated 200-mesh copper grids and stained with 2 % (w/v) uranyl acetate followed by 2 % lead citrate. These were viewed using a Philips EM300 electron microscope at an accelerating voltage of 60 kV with a liquid nitrogen cold trap in place at all times.

RESULTS

Site Description. The spring was located within a narrow ravine alongside a public hiking trail. Its source was surrounded by a corroded metal culvert (1.2 m diameter) in a vertical position so that its upper edge was flush with the surrounding soil, forming a small pool. A round plastic cover originally meant to cover the pool was present and had fallen within the opening so that part of its edge was visible as it sloped down into the pool at an angle of approximately 80°. This is the region of the spring which we will subsequently refer to as the source. The source was choked with leaves and with abundant microbial mats which nevertheless allowed water to flow freely over the lip of the pool at a rate of approximately 40 cm/s and down along the bottom of the ravine. The water flowed from the source year round with a constant temperature of 9°C and pH 7.1. An estimate of redox potential, using a hydrogen electrode, gave a reading of -335mV only 8 cm below the water surface.

Within the source, mass accumulations of microorganisms occurred as green, pink, and brown-green mats. The colours of the mats from different regions within the spring were due to the dominant microorganisms present in those regions. Due to the strong flow of the spring water, stratification in the mats was within masses rather than as straight and extensive laminations as has been noted for other microbial mats (D'Amelio et al. 1989; Douglas and Beveridge, 1998). Layering was only seen where the mats contacted the spring's bounding walls near the surface. Pink mats were dominated by purple sulfur bacteria while green-brown mats were dominated by green sulfur bacteria,

blue-green mats by cyanobacteria, and white mats (which grew in the channel beginning immediately downstream from the source) by colourless sulfur oxidising bacteria.

Microorganisms and patterns of sulfur accumulation; (a)colourless sulfur oxidising bacteria. In the Ancaster sulfur spring, both filamentous and unicellular colourless sulfur oxidising bacteria were present, particularly in the white mats downstream from the source. It was difficult to distinguish the small unicellular forms from the massive accumulations of S° present in their vicinity and which they deposited. Their presence was confirmed by observing, by light microscopy, bottled downstream spring samples in the laboratory over time. When the water began to lose its white opacity, due to use of accumulated S° by the cells as H_2S wasdepleted, light microscopy revealed small coccoid to rod-shaped cells, often with small spherical sulfur globules attached to them. The numerous cells seen in each field of view were of a similar size and shape and showed the same tendency to associate with the sulfur granules. Therefore they were presumed to be predominantly unicellular colourless sulfur oxidising bacteria.

Filamentous colourless sulfur oxidising bacteria were abundant in the downstream mats and in some of the pink-white mats collected from the surface regions of the source. By both ESEM (Figure 1) and light microscopy, the filaments appeared aseptate and were filled with numerous spherical sulfur inclusions of varying size along their entire length with a diameter of 1.5 to 2 μm and lengths too great to allow the ends of filaments to be seen among the mass accumulations of other organisms in the mats. These structural characteristics were similar to members of the genus *Thiothrix* (Nelson et al. 1989) or possibly *Thioploca* as described by (Jørgensen and Gallardo 1999). It was not possible to see whether the filaments possessed 'holdfast' structures at one end like the former genus but TEM observations (not shown) did show that sometimes more than one filament occurred within

a common sheath; a characteristic of *Thioploca* spp. Future studies may reveal that these are new members of a known genus of filamentous colourless sulfur oxidising bacteria.

EDS probing (Figure 2) of the intracellular spheres revealed that they were predominantly (95-98%) sulfur, the rest being made up of Fe (2 to 3%) and trace amounts of Ca, Si, Al, Mg (Table One) which could arise from stray signal due to nearby mineral grains. It was possible to get an intracellular signal because at the beam current and sample density used, the beam penetration was sufficient to pierce the cell and gain information from its interior.

(b) Green sulfur bacteria. Green sulfur bacteria were dominant in brown-green mats collected from all depths in the source but were absent from the white downstream mats. Samples thus known to be rich in green sulfur bacteria revealed large numbers of long sinuous rod shaped bacteria which were nonmotile and tended to aggregate in large masses. By ESEM, cells of a similar shape and same relative size were associated with masses of spherical elemental sulfur particles which formed macroscopically visible white masses within the brown green mats (Figure 3). Sulfur particles were also seen associated with cyanobacteria of which only one filamentous type was recognisable. These cyanobacteria were ubiquitous throughout the source regions of the mats and were likely existing as anoxygenic H_2S -utilising phototrophs. Elemental analysis of the sulfur granules revealed a remarkably consistent composition of 95 to 98% sulfur, 2 to 3 % Fe, and the rest trace Ca, Mg, Al, and Si, very much like the intracellular inclusions from the filamentous colourless sulfur oxidising bacteria. The lack of a detectable phosphorus signal indicated that these were not small unicellular bacteria.

TEM observations of these samples revealed the presence of numerous long rod-shaped bacteria and shorter rods in chains of which the individual cells were abundantly covered in spinae

(Figure 4). Spined cells were of two types: Short rods, 0.8 to 1.0 μm diameter, which, by the presence of chlorosomes, were identified as green sulfur bacteria resembling *Chlorobium* and long cells 1.2 to 1.5 μm in diameter, in which chlorosomes may have been present but were difficult to see due to being closely appressed to the cell membrane. Their presence was revealed when cells were sectioned in a plane that passed just within the plasma membrane. These cells often possessed darkly staining polyphosphate granules and may be similar to members of the genus *Chloroflexus*. The average diameter of the spinae was different for each type; 37 ±2 nm for the *Chlorobium*-like cells and 28 ±2 nm for the long rods (n=20 for each). In each case the spinae tapered out slightly with distance from the cell and exhibited a large length range from 30 to 200 nm.

(c) Epicellular sulfur deposition. One of the most interesting observations made by ESEM and by light microscopy, was the appearance of sulfur-encrusted microbial filaments. These were abundant in the brown-green mats from the source and were very similar in overall dimensions to the long spined *Chloroflexus*-like rods described above. They appeared as highly refractile objects by light microscopy (Figure 5) and correlated well with the occurrence of spinae-covered bacteria in thin-sectioned material viewed by TEM (see Figure 4). By ESEM, the encrustations themselves appeared as radiating outgrowths that followed the length of the cells and showed varying degrees of crystallinity, ranging from rounded, knob-like encrustations to pointed, diamond-shaped crystals (Figure 6). This range of structures seemed to indicate a progression in their formation but may also be due to deposition by structurally different bacteria. The correspondence between structure and elemental content is shown by the x-ray maps (Figure7.). By EDS (see Figure 2), all proved to be high in S (55% to 65%) and with 10% to 12% Fe and 10% to 15% Si (see Table One). This composition was consistent for multiple analyses (15 different structures were analysed at 2 different

points each, along their length) and contrasted to the elemental composition of the other forms of biogenic sulfur noted in the mats; sulfur spheres (95% S, 3% Fe) and the intracellular sulfur inclusions (92-95% S and 2-3% Fe).

DISCUSSION

In environments with fluctuating H_2S levels, sulfur deposits likely serve as inorganic energy storage for use when H_2S becomes scarce. Under such conditions, many organisms can further oxidise this form of sulfur, ultimately to sulfate. In the Ancaster sulfur spring, there is a continuous supply of H_2S and this may be a factor in allowing large masses of elemental sulfur to occur over time. These masses may also have once been intracellular sulfur which was liberated when the cell enclosing it died and was ruptured. The dynamics of such particles are not well known so it is difficult to speculate how long they may persist in the environment or what mechanisms may be involved in their dissolution/dispersal other than the microbial one mentioned above or physical disruption and transport downstream by the spring water.

Most of the unicellular colourless sulfur oxidising bacteria and some of the filamentous ones as well as most green sulfur bacteria are known to deposit elemental sulfur as extracellular spheres or ellipsoids, sometimes attached to the cell surface (Kuenen and Budecker 1982). Careful chemical and microbiological studies of intracellular sulfur inclusions have revealed that such deposits are not pure sulfur but have associated organic constituents. These are most likely in the form of a bounding layer of protein and/or lipid. In addition, it is likely that the sulfur inclusions are of a fluid-filled vesicular type made up of polythionates rather than a filled structure (Steudel 1989). It is not certain how extracellularly-deposited sulfur may compare chemically to its intracellular counterpart. In our

study, ESEM-EDS analysis revealed that the spherical extracellular sulfur was hydrophilic (unlike pure sulfur) as seen by its response to changing hydration levels in the ESEM, and that it had a small amount of Fe (2 to 5%) ubiquitously associated with it. In addition, when the energy of the electron beam was concentrated on these structures (such as during EDS analysis) they were disrupted by shrinkage or by beam penetration, leaving a small hole. These observations support the model (Steudel 1989) of bacteriogenic sulfur as a hydrated, possibly vesicular structure.

Possible role of spinae in elemental sulfur deposition. Spinae are made up of helically-arranged protein molecules which form hollow structures that protrude from the bacterial surface (Easterbrook and Coombs 1976). Our experience indicates that they tend to be seen on bacteria from natural, generally "extreme" environments, that they are common on the green sulfur bacteria in the Ancaster sulfur spring, and that they may be lost upon laboratory cultivation of bacteria. Spinae have been previously noted to occur on a range of different bacterial types such as marine pseudomonads (Easterbrook et al. 1973), green anoxygenic phototrophic bacteria (Cohen-Bazire et al. 1964; Stolz 1991; Brooke et al. 1992), and cyanobacteria (Perkins et al. 1981) and a number of different functions have been postulated. These include flotation (Perkins et al. 1981), spatial separation between cells, aggregation (1McGregor-Shaw et al. 1973), and predation avoidance (Sorokin and Carpenter 1981; Brooke et al. 1995).

One very pertinent study (Pibernat and Abella 1996) using the green sulfur bacterium *Chlorobium limicola* UdG 6083 noted a correlation between the amount of spinae per cell and the levels of H_2S in the cells' environment. When cells were given a constant supply of H_2S , they were unspined but when they experienced fluctuations in H_2S levels such that they underwent periodic H_2S starvation periods, they were abundantly spined and accumulated extracellular sulfur. This took the

form of spheres which attached to the cell surface. The authors concluded that the spinae, plus an extensive capsule, provided an attachment point for accumulation of sulfur. This then acted as an inorganic energy source so that the cells could oxidise it when H_2S levels became low. The cutoff point for H_2S levels was 400 μM (the H_2S level in the Ancaster sulfur spring is 3800 μM; S. Douglas, unpub.). However, they had no direct observations to support this hypothesis since the electron microscopical techniques they applied to their samples resulted in the destruction of the sulfur deposits. The results of our study appear to substantiate these earlier findings; spinae can act as accumulation sites for extracellular sulfur.

An interesting facet of this epicellular sulfur is its difference in elemental composition from that of the intracellular inclusions of the filamentous colourless sulfur oxidising bacteria and the spheres present as mass accumulations in the mats (see Table One). The consistently higher Fe and lower S content of the deposits seemed to indicate that some selective accumulation may have been occurring. Fe levels in the Ancaster sulfur spring are fairly low (2.87×10^{-3} mM in mat pore water; S. Douglas, unpub.) as compared to the sulfide levels so that in order to get the proportions seen in the epicellular deposits, there had to be a net accumulation of Fe from the spring water. Bacterial surfaces are well known to be potent scavengers of dilute metal ions in the environment (Schultze-Lam (Douglas) et al. 1993) and it has been suggested that spinae from a *Chlorobium* species in an oligotrophic freshwater lake may selectively accumulate Fe (J. Thompson, pers. comm.). It is possible that, in the Ancaster sulfur spring mats, the spinae-covered microorganisms accumulate Fe by binding to the cell surface and/or adsorption to the biogenic sulfur.

CONCLUSION

One of the most remarkable discoveries in our samples was the observation of sulfur-

encrusted cells and their correlation to spinae-covered bacteria seen in TEM thin sections. These forms were also readily seen by light microscopy, which we used to screen all our samples for electron microscopy. This allowed us to establish the dominant structural types in all the samples examined and therefore to correlate the results obtained with the various microscopical techniques. The spinae-covered bacteria seen by TEM are very likely the organisms seen to be covered by sulfur deposits and the appearance of these encrusted cells by ESEM gives the strong impression that spinae are the sites of deposition for the elemental sulfur on the cell surface. The use of ESEM has allowed us to gain information from our samples which was not previously obtainable in such a direct, reproducible, and detailed manner. As such, this this type of microscopy is an important tool in examinations of natural microbial communities. At present we are continuing our studies in the Ancaster sulfur spring by conducting phylogenetic analysis of the community and geochemical analyses to complement our extensive microscopical data.

ACKNOWLEDGEMENTS

Transmission electron microscopy was performed at the Guelph Regional NSERC Stem Facility which is supported by funding from the Natural Sciences and Engineering Research Council of Canada and is supervised by Dr. Terry Beveridge. We would also like to thank Jeff McLean for help in collecting samples. All work performed at JPL was supported by the Astrobiology section of the NASA Origins Program.

REFERENCES

Brooke, J.S., J.B. Thompson, T.J. Beveridge, and S.F. Koval. 1992. Frequency and structure of spinae on *Chlorobium* spp. Arch. Microbiol. 157:319-322.

Brooke, J.S., S.F. Koval, and T.J. Beveridge. 1995. Unusually stable spinae from freshwater *Chlorobium* sp. Appl. Environ. Microbiol. 61:130-137.

Cohen-Bazire, G., N. Pfennig, and R. Kunisawa. 1964. The fine structure of green bacteria. J. Cell. Biol. 22:207-225.

D'Amelia, E.D., Y. Cohen, and D.J. Des Marais. 1989. Comparative functional ultrastructure of two hypersaline submerged cyanobacterial mats: Guerrero Negro, Baja California Sur, Mexico, and Solar Lake, Sinai, Egypt, p. 97-113. *In* Y. Cohen, and E. Rosenberg (ed.), Microbial Mats: Physiological Ecology of benthic Microbial communities. ASM Washington D.C.

Douglas, S. and T.J. Beveridge. 1998. Mineral formation by bacteria in natural microbial communities. FEMS Microbiol. Ecol. 26:79-88.

Douglas. S. and D.D. Douglas. in prep. Ultrastructure and geomicrobiological relations of a cold sulfide spring microbial community from Ancaster, Ontario, Canada.

Easterbrook, K.B., J.B. McGregor-Shaw, and R.P. McBride. 1973. Ultrastructure of bacterial spines. Can. J. Microbiol. 19:995-997.

Easterbrook, K.B., and R.W. Coombs. 1976. Spinin: the subunit protein of bacterial spinae. Can. J. Microbiol. 23:438-440.

Jørgensen, B.B. and Y. Cohen. 1977. Solar Lake (Sinai). 5. the sulfur cycle of benthic cyanobacterial mats. Limnol. Oceanogr. 22:657-666.

Jørgensen, B.B., and V.A. Gallardo. 1999. *Thioploca* spp.: filamentous sulfur bacteria with nitrate vacuoles. FEMS Microbiol. Ecol. 28:301-313.

Kuenen, J.G., and R.F. Budeker. 1982. Microbiology of thiobacilli and other sulfur-oxidising autotrophs, mixotrophs, and heterotrophs. Phil. Trans. Royal Soc. London B. 293:473-497.

McGregor-Shaw, J.B., K.B. Easterbrook, and R.P. McBride. 1973. A bacterium with ehinuliform (nonprosthecate) appendages. Int. J. Syst. Bacteriol. 23:267-270.

Nelson, D.C., C.O. Wirsen, and H.W. Jannasch. 1989. Characterisation of large, autotrophic *Beggiatoa* spp. abundant at hydrothermal vents of the Guaymas Basin. Appl. Environ. Microbiol. 55:2909-2917.

Perkins, F.O., L.W. Haas, D.E. Phillips, and K.L. Webb. 1981. Ultrastructure of a marine *Synechococcus* possessing spinae. Can. J. Microbiol. 27:318-329.

Pibernat, I.V., and C.A. Abella. 1996. Sulfide pulsing as the controlling factor of spinae production in *Chlorobium limicola* strain UdG 6038. Arch. Microbiol. 165:272-278.

Schultze-Lam, S., J.B. Thompson, and T.J. Beveridge. 1993. Metal ion immobilisation by bacterial surfaces in freshwater environments. Water Poll. Res. J. Canada. 28:51-81.

Sorokin, D.J., and E.J. Carpenter. 1981. Cyanobacterial spinae. Botanica Marina 24:389-392.

Steudel, R. 1989. On the nature of "elemental sulfur" (S^0) produced by sulfur-oxidising bacteria-a model for S^0 globules, p. 289-303. *In* H.G. Schlegel (ed.), Autotrophic Bacteria. Elsevier, Amsterdam.

Stolz, J.F. 1991. Structure of phototrophic prokaryotes. CRC Press, London.

Table One. Typical EDS Quantitative Analyses for Representative Sulfur-Bearing Structures in Mats from the Ancaster Sulfur Spring

	Element, Proportion (%)[A]								
Sample	S	Fe	Si	Ca	Mg	Zn	Al	P	Description[B]
ddss1	95.1	2.5	0.9	0.8	0.1	0.1	0.5	0	intracellular
ddss2	91.2	3.3	1.9	1.4	0.4	1.1	0.7	0.1	intracellular
ddss3	95.0	2.1	0.9	0.3	0	1.6	0.2	0	intracellular
ddss8	93.9	4.7	0.2	0.1	0.2	0.2	0.4	0.4	intracellular
ddss4	95.1	2.2	0.6	0.3	0.1	1.4	0.4	0	sphere in mass
ddss5	95.2	2.3	0.8	0.4	0	0.8	0.5	0	sphere in mass
ddss6	94.6	2.5	0.5	0.6	0.2	1.5	0.1	0	sphere in mass
ddss12	91.5	1.8	4.3	0.8	0.2	1.1	0.3	0	sphere in mass
14991	90.7	3.7	3.3	1.3	0.1	0	1	0	epicellular
149910	84.2	6	3.6	5.2	0.2	0	0.9	0	epicellular
14994	87.7	5.9	3.2	1.7	0.5	0	1	0	epicellular
14995	90.4	5.2	2	1.2	0.3	0	0.9	0	epicellular
14996	70.6	12.5	8.6	2.4	1.2	1.9	2.6	0.3	epicellular
14998	87.2	6.8	3.0	1.5	0.3	0	1.1	0	epicellular
14999	84.8	8.4	3.4	1.5	0	0.5	0.8	0	epicellular
149912	33.2	21.9	23.9	10.1	1.5	0.4	8.9	0.2	mineral
14997	27.3	12.4	45.5	2.6	1.5	0.3	10.5	0	mineral

[A]The EDS results are given as atomic proportions, in %, of a given sample and have an error of ±0.1%.
[B]intracellular = sulfur inclusions of filamentous colourless sulfur bacteria; sphere in mass = extracellular spherical biogenic sulfur particles formed by grren, bacteria, colourless sulfur bacteria, and cyanobacteria; epicellular = encrusted filaments which showed a shape variation of sulfur from rounded to angular radiating crystals covering the cell surface; mineral = silicate mineral grains, possibly clays, commonly found as sediment in the spring channel and within mats from the source.

FIGURE LEGENDS

Figure 1: These ESEM images show the typical appearance of filamentous colourless sulfur oxidising bacteria when viewed using this microscopic method. The filaments are electron translucent, except for the internal sulfur granules (S) which show up as spheres or ovoids along the entire length of the filaments. The cyanobacteria (Cb) coexisted with these forms also, since they were ubiquitous in all lighted regions of the spring. These organisms had interesting small inclusions lined up along cell septa (arrows in **B**) which gave a high sulfur signal relative to the rest of the cell.

Figure 2: Energy dispersive x-ray spectroscopy (EDS) spectra of representative samples from the source mats. The top spectrum (**A**) is representative of all the putative bacteriogenic sulfur deposits; the intracellular granules, extracellular spheres, and epicellular deposits. The lower spectrum (**B**) is typical of the silicate mineral grains, possibly clays, which were commonly occluded within the mat material. The sulfur peak is likely due to the presence of abundant bacteriogenic sulfur. Likewise, the non-sulfur peaks in **A** are due to the presence of nearby mineral grains. The maximum peak heights are 7000 counts for S in **A** and 1500 counts for Si in **B**.

Figure 3: ESEM images of extracellularly-deposited sulfur spheres. In **A**, a mass deposit of sulfur spheres (S) clings to numerous cyanobacterial filaments (Cb) in mats from the spring source. In the Ancaster sulfur spring cyanobacteria lived throughout the anoxic zones of the spring and must rely on anoxygenic photosynthesis as an energy generating mechanism. In some areas of the image, the extensive gel-like matrix of extracellular polymeric substance (E) is visible, with individual sulfur spheres embedded within it (arrow). **B**: Sometimes, the sulfur accumulations were very extensive. EDS analysis of suh large masses failed to give a phosphorus signal, indicating that these were not small bacterial cells. Occasionally, some of the spheres, appeared to have irregularities, reminiscent of dents in their surfaces (arrow). These may give credence to the idea that bacteriogenic sulfur has

C-E: These three images show the progressively more spiky appearance of the epicellular sulfur deposits from knobby (**C**) to spiky (**E**). The differing appearances may represent different stages in formation of the deposits or may be due to differences in the underlying bacterial structure. **F:** Detailed view of a sulfur-encrusted filament. The underlying material is the filter paper upon which the mat samples were laid for viewing in the ESEM. **G:** Magnified view of a portion of the filament shown in **F**. At the sites marked by arrows, the spikes appear to be made up of tiny individual spheres, a possible clue to their formation.

Figure 7: ESEM-EDS x-ray maps of sulfur-encrusted bacteria from the source mats. **A:** Image produced by using all xray wavelengths generated by the sample using a 20 keV accelerating voltage. **B:** Image produced using only the sulfur elemental lines. Some of the features seen in the full spectrum image (see arrows in **A**) are no longer visible, since they contain no sulfur. Comparison of the two images can reveal many more features not visble in the sulfur image. **C:** This phosphorus image shows the regions in which P is concentrated. This element is found in detectable amounts only in microbial cells in these samples. This shows that the sulfur structures must be encrusted bacteria, rather than an abiological phenomenon.

a vesicular, fluid filled structure.

Figure 4: Images of 70-nm thin sections from the brown-green source mat. This is the same sample in which sulfur-encrusted bacterial filaments were abundant. By TEM, the most numerous organisms were spined cells such as those shown here. The spinae (40 to 70 nm diameter) can be seen protruding from the cell surface and their helical pattern of construction is evident, especially on the cell in **A**. All the cells have Gram negative cell envelope profiles with at least one (shown in **C**) being identifiable as a green sulfur bacterium by its peripherally located electron translucent chlorosomes. Some green sulfur bacteria do not have obvious photosynthetic membrane structures and it is possible that these are represented in the other three images. By correlation with light microscopic and ESEM views of the same sample, it is likely that these spined cells are the same as those which show epicellular sulfur deposition.

Figure 5: These phase contrast microscopic images show the different overall structures of the sulfur-encrusted bacterial filaments. In **A** a fully developed "spiky" filament with radiating sulfur-encrustations can be seen. One end of the filament is embedded in the brown-green mat material from the spring's source, in which these forms were most commonly seen. **B:** A "smooth" encrusted filament. At certain points along its length, more crystalline, often diamond-shaped sulfur deposits are seen (arrows). **C:** A shorter encrusted filament showing that the radiating spikes are more pointy than in the variant shown in **A.**

Figure 6: ESEM images of fully hydrated sulfur-encrusted bacteria from the source mats. **A:** Overview of a mat sample in which the encrusted bacterial filaments are common; these are the long structures, often spiny-looking, in this image. Note the silicate mineral grain in the centre of the image. **B-G:** Detailed views of sulfur-encrusted filaments. In **B**, A spiky filament is seen together with a smoother, "knobby" one, showing the different degrees of encrustation exhibited by the filaments.

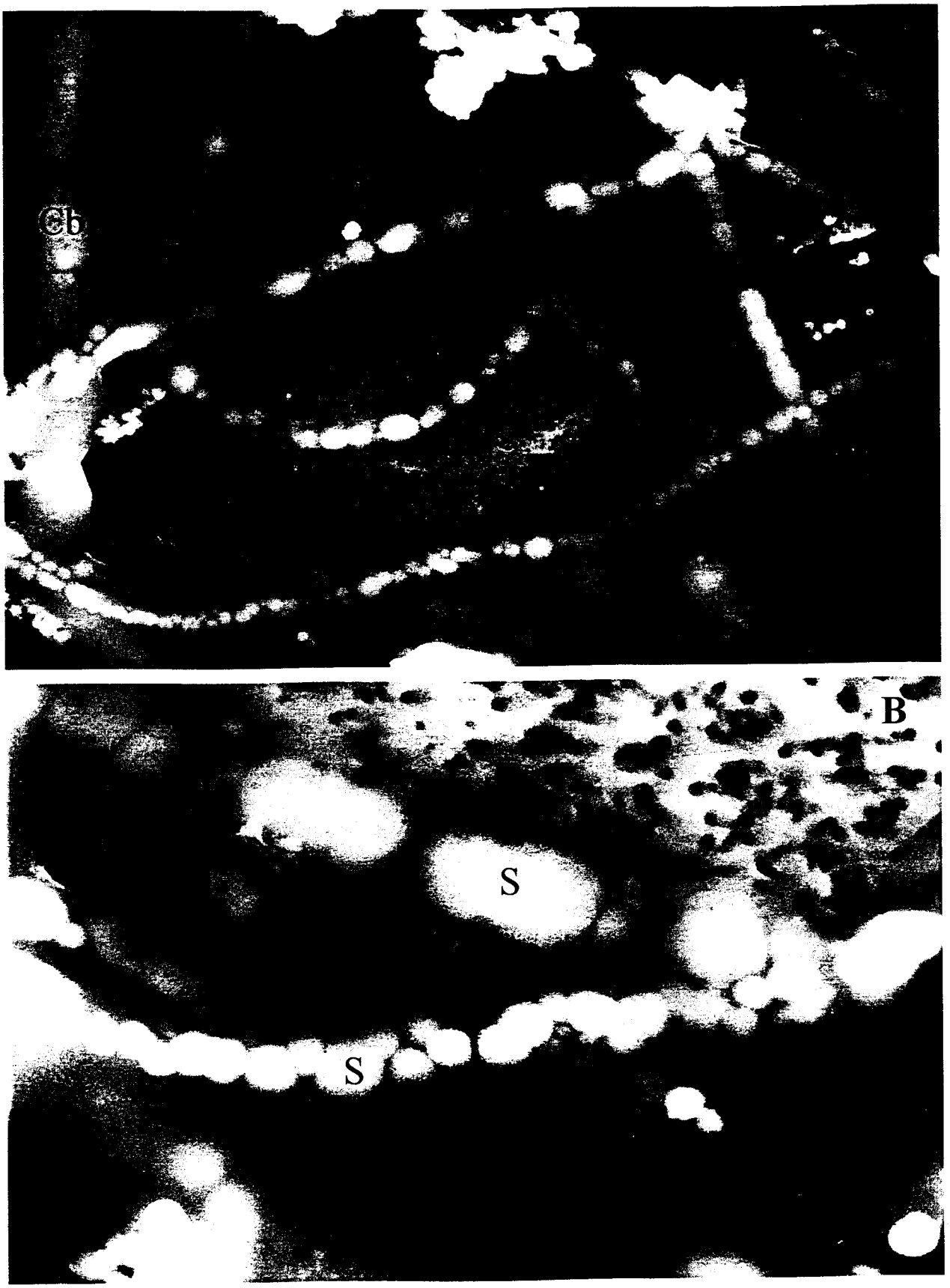
b
B
S
S

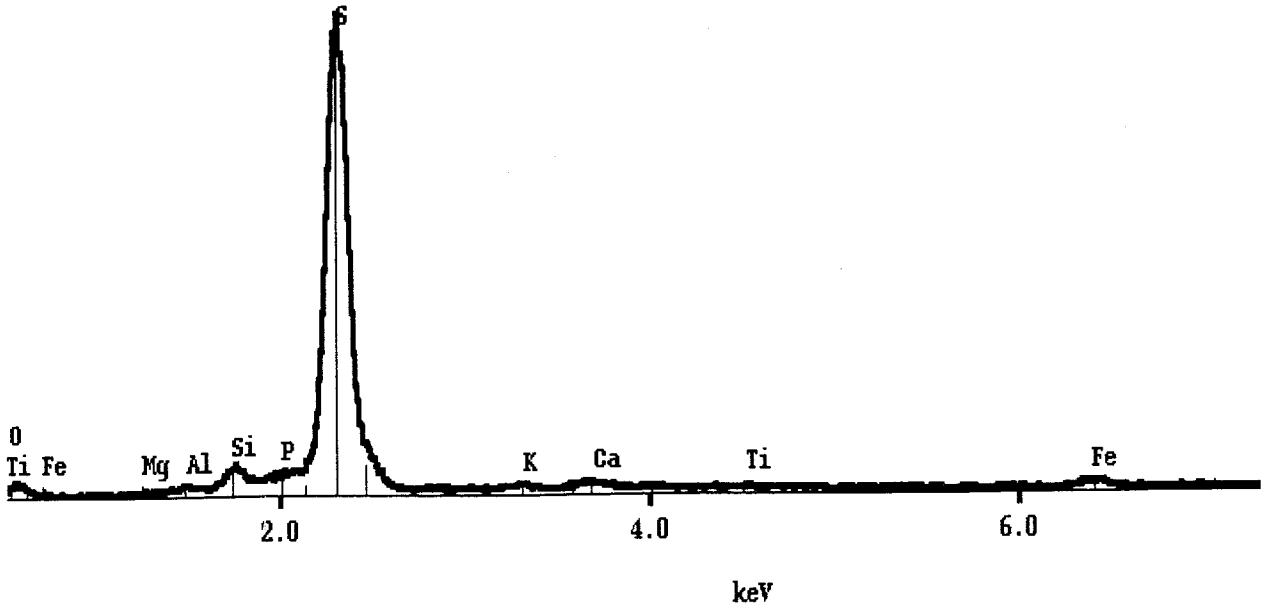
O
Ti Fe
Mg
Al
Si
P
S
K
Ca
Ti
Fe
2.0
4.0
6.0
keV

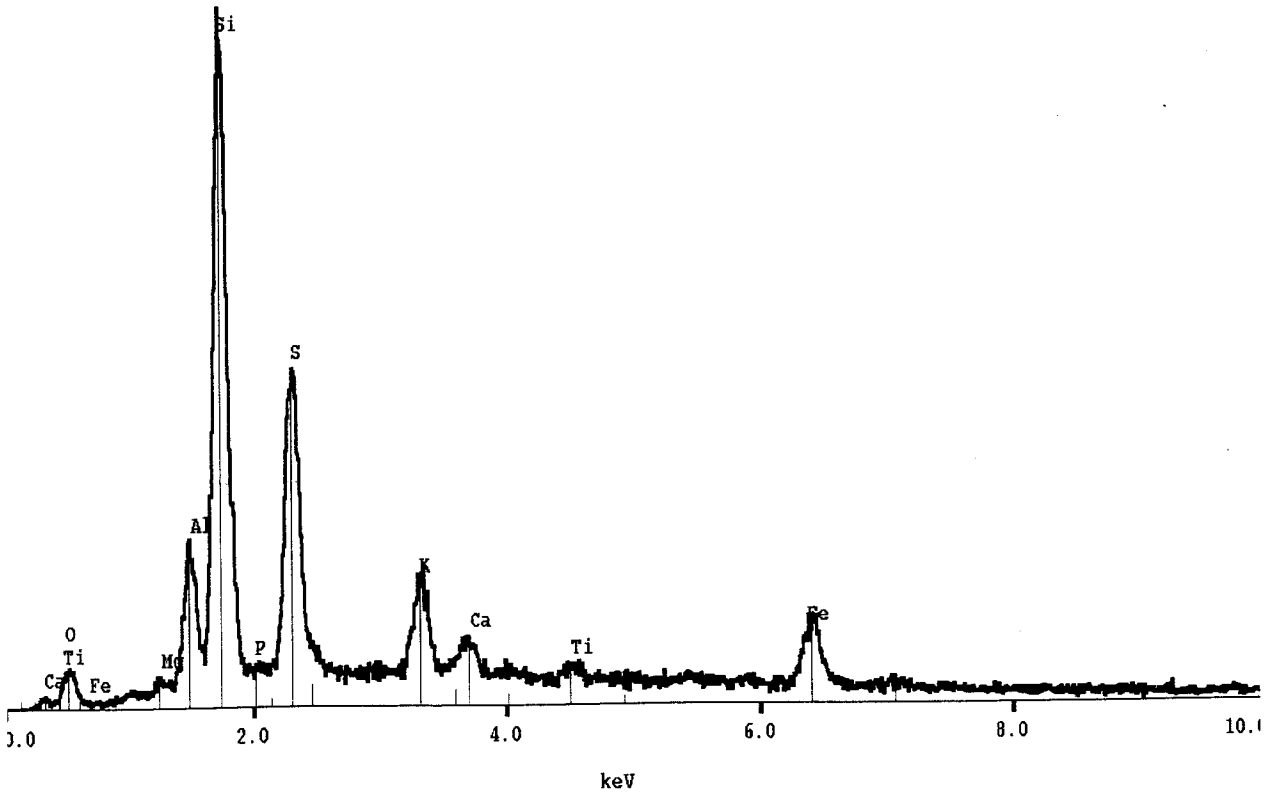
Si
S
Al
K
Ca
Ti
Fe
O
Ti
Ca
Fe
Mg
P
2.0
4.0
6.0
8.0
keV

S
B

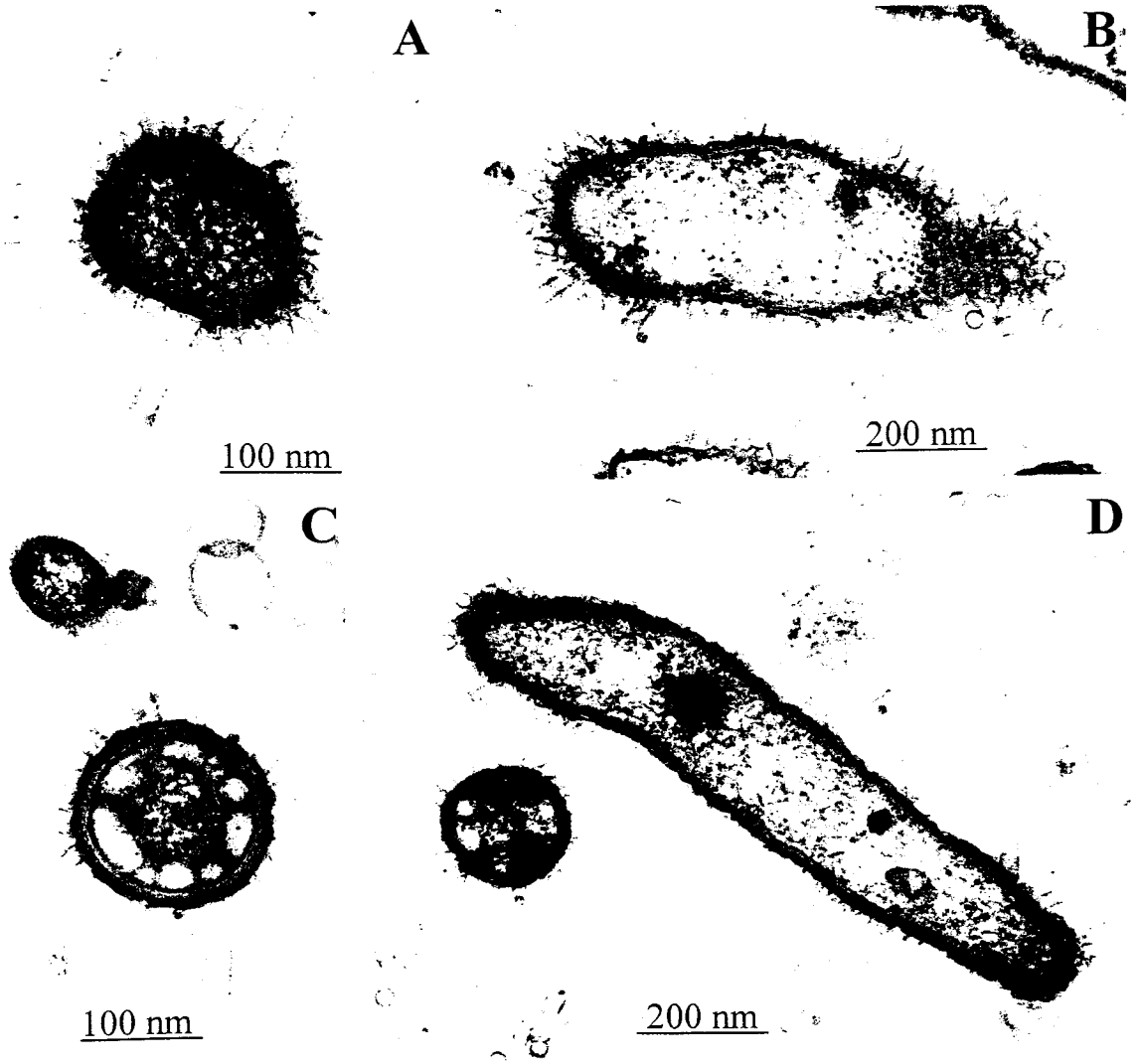
A
B
100 nm
200 nm
C
D
100 nm
200 nm

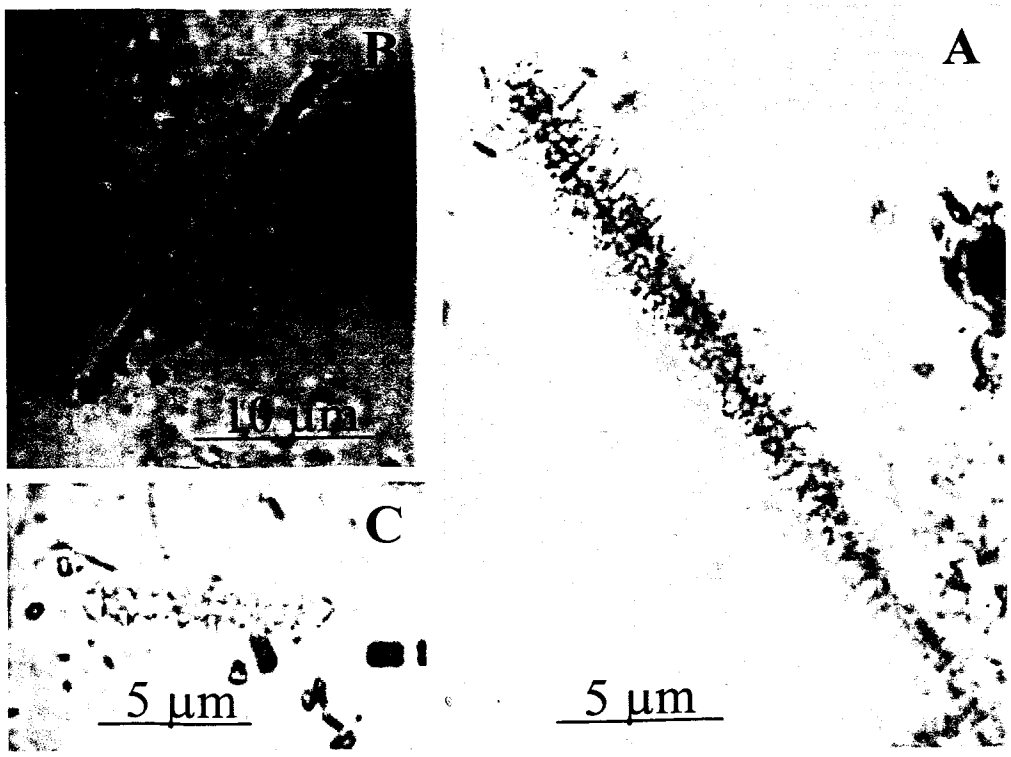
B
10 µm
C
5 µm
A
5 µm

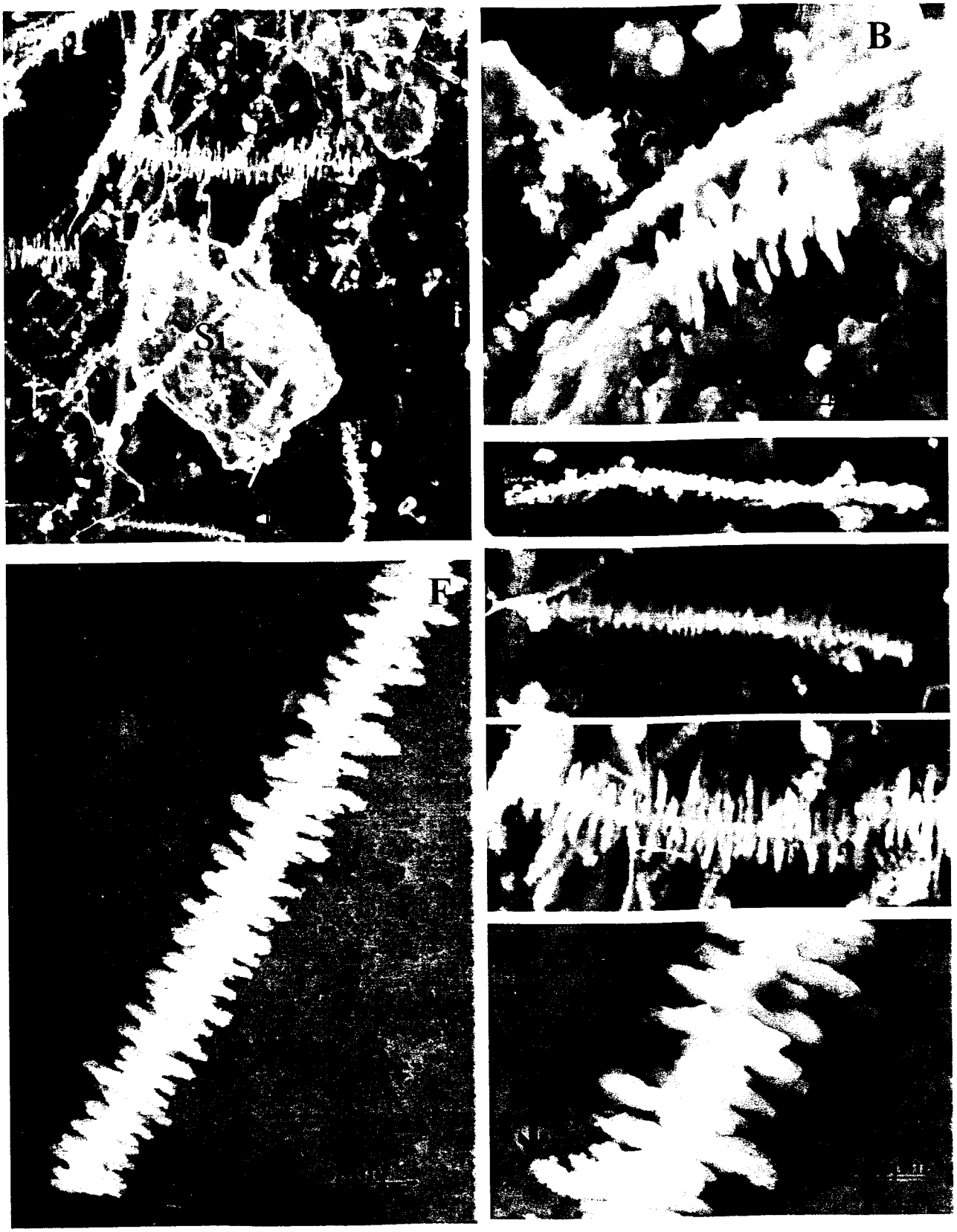
B
F